Tetrahedron 78 (2021) 131830

Contents lists available at ScienceDirect

Tetrahedron

journal homepage: www.elsevier.com/locate/tet

Diastereoselective synthesis of new Thiazolyl-Indazole derivatives from *R*-carvone: A combined experimental and theoretical study

A. N'Ait Ousidi [a], M.Y. Ait Itto [a], A. Auhmani [a], M. Loubidi [a], A. Riahi [b], J.-C. Daran [c], M. Esseffar [a], Carol A. Parish [d, *]

[a] Département de Chimie, Faculté des Sciences Semlalia, Cadi Ayyad University, BP 2390, Marrakech, Morocco
[b] Institut de chimie moleculaire de Reims (ICMR), CNRS UMR 7312 UFR Sciences, University of Reims, B.P. 1039, 51687, REIMS Cédex 2, France
[c] Laboratoire de Chimie de Coordination du CNRS, 205 Route de Narbonne, 31077, Toulouse Cedex 04, France
[d] Department of Chemistry, University of Richmond, Gottwald Center for the Sciences, Richmond, VA, 23173, USA

ARTICLE INFO

Article history:
Received 7 October 2020
Received in revised form
25 November 2020
Accepted 28 November 2020
Available online 3 December 2020

Keywords:
Thiosemicarbazones
1,3-Thiazole
Indazole
Diastereoisomers
NMR
X-ray crystal structure
Density functional theory (DFT)

ABSTRACT

The reaction of (R)-carvone and (R)-pulegone thiosemicarbazones with phenacyl bromide yields two new thiazoles: (*R*)-2-(2-(5-isopropyl-2-methylcyclohex-2-enylidene) hydrazinyl)-4-phenylthiazole, ***I*** and (*3aR,6R*)-3,3,6-trimethyl-2-(4-phenylthiazol-2-yl)-3,3a,4,5,6,7-hexahydro-2H-indazol-3a-ol, ***II***, respectively. While HRMS and NMR spectroscopic data confirm the expected structure of ***I***, they show that the product from (R)-pulegone undergoes rearrangement and oxidation to give ***II***. The orientation of the OH group in ***II*** produces two possible diastereoisomers; (3a*R*,6*R*) and (3a*S*,6*R*). X-Ray analysis was used to assign the (3a*R*,6*R*) configuration to ***II***. Energetic analysis with the M052-X functional with 6-31+G(d,p) basis set showed that the (*3aR,6R*) is more stable than the (*3aS,6R*) diatereoisomer by approximately 4.5 kcal/mol. The dimerization of the (*3aR,6R*) isomer of ***II*** was studied computationally via two types of hydrogen bonding interactions: (OH···O), as the conventional hydrogen bonding, and the interaction of the OH group with the aromatic ring (OH···Ar). We find that these two modes of polymerization are approximately isoenergetic.

1. Introduction

In recent decades, nitrogen and sulfur-containing aromatic heterocycles have attracted great attention owing to their interesting pharmacological activities and industrial importance. Particularly, thiazoles are a familiar group of heterocyclic compounds possessing a wide variety of biological activities, and their utility in drug design is well established. The thiazole nucleus is a basic feature of vitamin B1 and luciferin produced by fireflies. Thiazole derivatives have been shown to have applications as biocides [1], anticorrosive fuel additives [2], and antioxidants [3].

Indazoles are also of particular significance as a large number have shown enhanced biological activities. Indazoles are not commonly found in natural products; however, several recent studies have reported the synthesis of new indazolic compounds [4–8]. Indazole-based compounds are playing an increasingly important role in the development of medicinal chemistry as they show a broad spectrum of biological activities and have found roles as analgesic, antipyretic, anticancer, antiarthritic and antifungal drugs [9].

As a part of our endeavor towards the preparation of new heterocyclic systems from naturally occurring monoterpenes [10–14] we report, in the present paper, the synthesis and spectroscopic characterization of two new, optically active thiazoles ***I*** and ***II***, from thiosemicarbazones of naturally occurring (R)-carvone and (R)-pulegone, by heterocyclization reaction with phenacyl bromide. The newly obtained heterocycles were fully characterized by their HRMS and NMR spectroscopic data reported herein. We also report an X-ray analysis and a computational study at the M05-2X/6-31+G(d,p) level to elucidate the unexpected structure of ***II*** and explain its formation as a ***(3aR,6R)*** diastereomer. To understand the polymerization observed experimentally by X-ray crystallography, two types of interactions were considered: the conventional (OH···O) and non-conventional (OH···Ar) [15] hydrogen bond in gas phase and in ethanol as solvent.

* Corresponding author. Department of Chemistry, Gottwald Center for the Sciences, University of Richmond, Richmond VA, USA.
E-mail address: cparish@richmond.edu (C.A. Parish).

https://doi.org/10.1016/j.tet.2020.131830
0040-4020/

2. Results and discussion

2.1. Synthesis and characterization

The synthesis of (R)-2-(2-(5-isopropyl-2-methylcyclohex-2-enylidene) hydrazinyl)-4-phenylthiazole ***I***, and (*3aR,6R*)-3,3,6-trimethyl-2-(4-phenylthiazol-2-yl)-3,3a,4,5,6,7-hexahydro-2H-indazol-3a-ol ***II***, was achieved by heterocyclization reaction starting from thiosemicarbazone **2** and **3** respectively (Scheme 1). These species were condensed separately with phenacyl bromide **1**, in the presence of sodium acetate in refluxing ethanol. A proposed mechanism for the cyclization of **2** with **1** to form **I** is shown in Scheme 1S of the Supporting Information.

The 1,3-thiazole ***I*** was further purified by liquid chromatography using hexane/ethyl acetate gradient as eluent to yield analytically pure products (98%). The structure was fully elucidated using high resolution mass spectrometry (HRMS) and nuclear magnetic resonance (NMR) spectroscopy.

The ES-HRMS spectrum of ***I*** shows a pseudomolecular ion $[M+H]^+$ at $m/z = 324.1530$ consistent with the molecular formula $C_{19}H_{21}N_3S$, while its infrared spectrum exhibits a strong band at 3416 cm^{-1} and a weak band at 1496 cm^{-1} characterizing the N-H group of a secondary aromatic amine in its both stretching and scissoring vibrational modes. In the ^1H NMR spectrum of ***I***, we noticed the disappearance of the three signals at 9.12, 7.31 and 7.16 ppm which distinguished the thioureido group of the starting thiosemicarbazone **2**, along with the appearance of the thiazolic proton as a singlet at 6.82 ppm. The product ***I*** was further confirmed by the appearance of five aromatic protons of the phenyl group resonating as three separate signals: a doublet ($J = 7.5$Hz) due to two protons at 7.70 ppm, a triplet (J = 7.5Hz) ascribed to two protons at 7.26 ppm, and single proton multiplet at 7.21 ppm. The NH proton, exchanged with D_2O, was observed at 10.81 ppm as a broad signal (Fig. 1S).

The carvone skeleton of ***I*** was confirmed by its five basic signals: a broad singlet at 5.92 ppm due to the endocyclic double bond proton, two separate singlets at 4.44 and 4.60 ppm assigned to the two ethylenic protons of the exocyclic double bond and finally two other singlets observed at 1.92 and 1.55 ppm attributed to the two methyl groups (Fig. 1S).

The main evidence for the 1,3-thiazole nucleus of ***I*** was apparent in the ^{13}C NMR spectra. The thiazolic H-Csp^2 carbon appeared at 103.47 ppm along with resonances for the two quaternary sp^2 carbons appearing at 157.89 and 146.27 ppm. The phenyl substituent was mainly depicted by three signals at 128.52, 127.57 and 126.06 ppm corresponding to H-Csp^2 carbons. On the other hand, the four carbon resonances appeared at 131.58 (H-$\underline{C}sp^2$), 132.53 (quaternary $\underline{C}sp^2$), 134.97 (quaternary Csp^2) and 109.94 ppm (H_2-$\underline{C}sp^2$) due to C=C double bonds. Taken together, these assignments are sufficient to characterize the carvone skeleton (Fig. 2S).

Condensation of (R)-pulegone thiosemicarbazone **3** with phenacyl bromide **1**, did not lead to the expected (R)-2-(2-(5-methyl-2-(propan-2-ylidene) cyclohexylidene) hydrazinyl)-4-phenylthiazole ***III***, but to the indazolic 1,3-thiazole ***II*** in 36% yield (Scheme 1). For this reaction to occur, **3** must rearrange via an intramolecular heterocyclization reaction involving N-H addition of the thioureido group to the C=C double bond. This rearrangement is known to occur before the condensation reaction with **1** and subsequent oxidation of the C-H bond at the ring junction to form the indazolic 1,3-thiazole ***II*** (Scheme 2). This is known to be readily accomplished in either acidic or basic media [14].

The structure of ***II*** was characterized using ES-HRMS and NMR spectroscopic techniques. The ES-HRMS spectrum exhibits a pseudomolecular ion $[M+H]^+$ at $m/z = 342.1635$ confirming a $C_{19}H_{23}N_3OS$ molecular formula, while its IR spectrum revealed a strong and sharp band at 3526.75 cm^{-1} corresponding to a free OH stretching vibration.

In the ^1H NMR spectra (Fig. 3S), the most salient features of ***II*** are the two singlets at 6.85 ppm and 1.94 ppm. The former is typical of the thiazolic proton and the latter is ascribed to the hydroxy proton, which is D_2O exchangeable. These two structural moieties were confirmed in the ^{13}C NMR spectra, by resonances of the thiazolic H-Csp^2 carbon and the sp^3 quaternary carbon of the carbinol group that appeared at 103.38 and 84.62 ppm, respectively. Furthermore, the lack of a chemical shift signal in the narrow range 126–132 ppm, which typically distinguishes the two quaternary

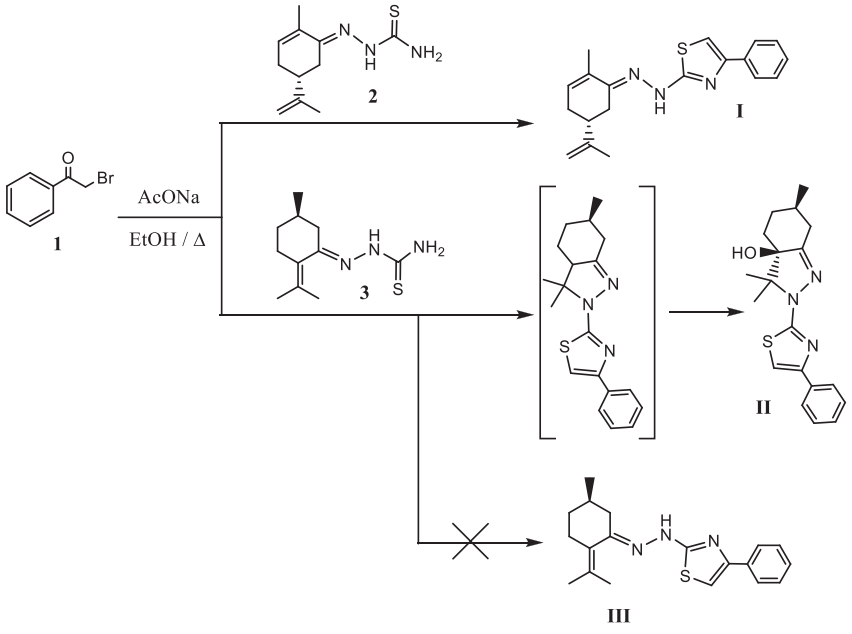

Scheme 1. Synthesis of I and II.

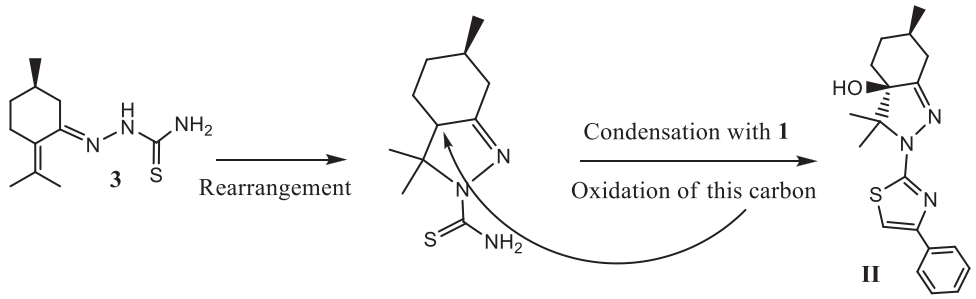

Scheme 2. Rearrangement of 3 to allow condensation with 1 to form II.

Csp^2 of the C=C double bond, and the appearance downfield of two new Csp^3 quaternary carbons at 84.62 and 70.40 ppm, confirms both rearrangement of the hydrazono-pulegone moiety into an indazole-like nucleus, and the oxidation of the C-H bond at its ring junction (Fig. 4S).

In the ^{13}C NMR spectra of ***II*** (acquired with H decoupling), we note no splitting of signals due to carbons near the newly formed asymmetric C3a carbon; this confirms the presence of only one diastereomer. In view of all these spectral data, the structure of ***II*** was unambiguously identified as 3,3,6-trimethyl-2-(4-phenylthiazol-2-yl)-3,3a,4,5,6,7-hexahydro-2H-indazol-3a-ol.
However, the absolute configuration of the newly formed asymmetric carbon at the ring junction remained unknown. This prompted us to carry out an X-ray crystallographic study of ***II***, aiming at both resolving its absolute configuration and confirming the entire structure.

2.2. X-ray crystal structure of II

Slow evaporation from an ethanolic solution of compound ***II*** gave crystals suitable for crystallographic analysis. A single crystal of ***II*** was mounted under inert perfluoropolyether at the tip of a glass fiber and cooled in the cryostream of a Nonius Bruker APEX II diffractometer [16]. Data was collected using the monochromatic MoKa radiation (k = 0.71073).

The structures were solved by direct methods (SIR97) [17] and refined by least-squares procedures on F2 using SHELXL-97 [18]. All H atoms attached to carbon were introduced in the calculation in idealized positions and treated as riding models. The absolute configuration (*3aR,6R*) has been unambiguously determined by the refinement of the Flack parameters [19] confirming the expected stereochemistry from the synthetic pathway. The drawings of the molecules were realized with the help of ORTEP32 [20,21]. Crystal data and refinement parameters are shown in Table 1S. The crystallographic data (CCDC 1563919) can be obtained free of charge from the Cambridge Crystallographic Data Centre via www.ccdc.cam.ac.uk/data_request/cif.

The ORTEP structure of ***II*** is shown in Fig. 1. Selected distances and angles are reported in Table 1S. The structure contains a pyrazole ring linked to a thiazole nucleus bearing a phenyl ring. The thiazole and phenyl rings are nearly planar making a dihedral angle of 3.82(6)°. The cyclohexane ring fused to the pyrazole displays a chair conformation with a puckering parameter θ = 163.8° whereas the five membered pyrazole ring adpots a half-chair conformation with ϕ = 254.05° (105.95) [22].

Intermolecular interactions are observed between molecules of ***II*** via non-conventional hydrogen bonding interactions between the hydroxyl OH group and the aromatic electron density of the thiazole attached phenyl ring, represented as the centroid of the symmetry related phenyl ring, as shown in Fig. 2. The crystal packing forces, driven by these O-H...Ar interactions, forms a helical chain developing along the b-axis. The distance between the H of each hydroxyl group and the centroid of the aromatic ring is 3.546 Å and the bond angle (O-H-Cg) is 169°. (Cg is the centroid of the C(6)···C(11) phenyl ring (Fig. 1)).

2.3. Evaluating the diastereomers of II, and dimer energetics

Geometry optimizations of the two diastereomers (*3aR,6R*) and (*3aS,6R*) of ***II*** in gas phase and in solvent were performed at the M05-2X/6-31+G(d,p) level of theory. The nuclear-plus-electronic and zero-point vibrational energies (ZPE) are summarized in Table 2S of the Supporting Information. Total and relative energies, including ZPE correctioins, in gas phase and in ethanol, are given in Table 1.

The (*3aR,6R*) diastereomer is 4.5 kcal/mol more stable than (*3aS,6R*). This enhanced stability is due to subtle differences in a variety of degrees of freedom, most notably in the dihedral angles near the 3αC as well as in the intramolecular hydrogen bonding interactions between the hydroxyl hydrogen and the lone pairs on the nitrogens in the indazol-like ring of ***II*** (Fig. 3). In the (*3aR,6R*) isomer the hydroxyl hydrogen forms a bifurcated interaction with both nitrogen atoms (2.87 Å and 2.73 Å) whereas in the (*3aS,6R*) isomer the hydroxyl is oriented more towards the nitrogen bonded to the thiazole ring (2.58 Å) relative to the nitrogen within the indazol-like ring (2.78 Å). These interactions are not much shielded by solvent, i.e. the relative energies of the (*3aR,6R*) and (*3aS,6R*) isomers are similar in solvent (4.6 kcal/mol in favor of (*3aR,6R*)). This result is consistent with the experimental (*3aR,6R*) crystal structure (Fig. 1).

Structural stability of the *3aR, 6R* dimer. The X-ray study suggests that ***II*** can readily polymerize via (O-H···Ar) packing interactions between the hydroxyl OH group and the phenyl ring. To better understand the energetics and atomistic details of the intermolecular interactions of the diastereomer, we performed calculations on the (*3aR,6R*) dimer in two different arrangements: i) optimizing the (OH···Ar) interactions between the OH group and the aromatic ring, and ii) optimizing the interaction between the OH groups (OH...O), as more commonly occurs in the classical polymerization of alcohols. A competition between (OH···O) and (OH···Ar) docking sites has recently been reported for several hydrogen bonded complexes [23–27]. It is also well known that the (OH···O) interactions are preferred for the polymerization of most alcohols in the absence of steric effects [28].

As shown in Fig. 4, the (OH···O) optimized dimer contains an (OH···O) intermolecular hydrogen bond of 1.98 Å. In this orientation, the approach of other molecules to the dimer for higher ordered polymerization is relatively hindered. However, in the case of the (OH···Ar) optimized dimer, the proton donating OH group approaches the aromatic ring forming a multifurcated hydrogen bond

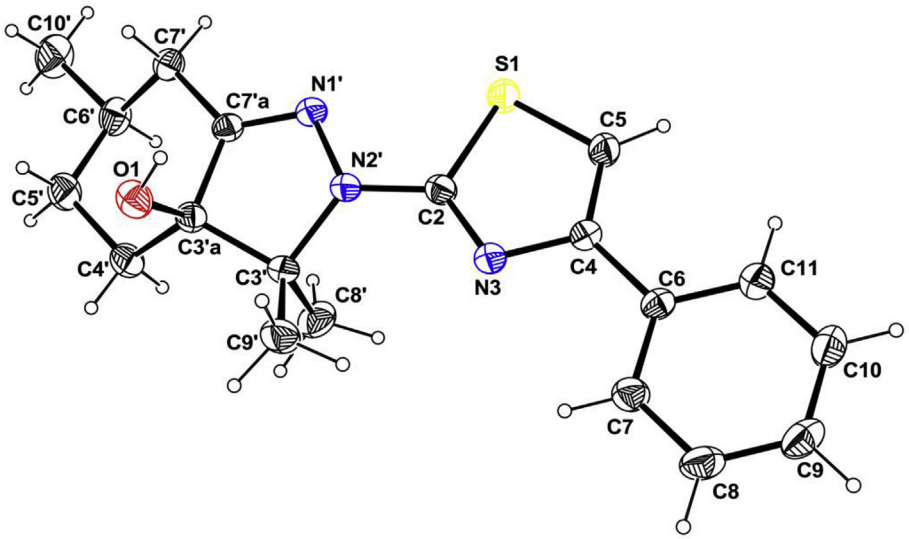

Fig. 1. ORTEP structure of II. Ellipsoids are drawn at the 50% probability level. H atoms are represented as small circles of arbitrary radii.

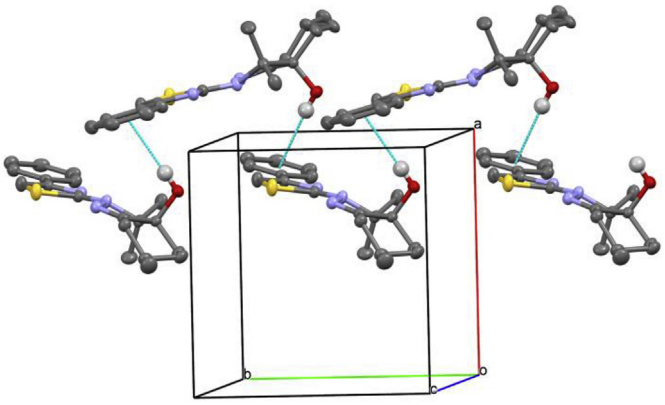

Fig. 2. Partial packing view showing the formation of a helical chain developing parallel to the b-axis.

Table 1
M052-X/6-31+G(d,p) total energies E (a.u) and relative energies ΔE(kcal/mol) of (3a*R*,6*R*) and (3a*S*,6*R*) diastereomers.

Diastereomer	Gas phase		Ethanol	
	E[a]	ΔE[b]	E[a]	ΔE[b]
(3aR,6R)	−1375.08953	- 4.5	−1375.10154	- 4.6
(3aS,6R)	−1375.08229		−1375.09418	

[a] Total energies are corrected by ZPE, which is scaled by the empirical factor of 0.961.
[b] ΔE = E((3aR,6R)-(3aS,6R)).

where the distance between the H atom of OH group and each carbon atom of the aromatic ring is about 2.70 Å. In this orientation, the molecules stack in parallel planes without any steric hindrance allowing the polymerization to occur easily.

The ZPE and BSSE-corrected dimer energies (Table 2) suggest that the (OH···O) and the (OH···Ar) oriented dimers are nearly isoenergetic in both the gas-phase and solvent (ethanol) environments (0.68 kcal/mol gas phase; 0.84 kcal/mol ethanol). While there is a small energetic preference for the (OH···O) oriented dimer, polymerization beyond the dimer is sterically constrained. Steric crowding is not observed in the (OH···Ar) and the likely reason why this orientation is observed experimentally.

QTAIM theory was also used to compare the two different modes of dimer interaction. The charge density (ρ) at the bond critical points (bcps) of the (OH···O) and (OH···Ar) isomers are depicted in Fig. 5. The values of the charge density at the bcps correlate well with the intermolecular bond distances: the shorter the bond, the larger the ρ value. It is noteworthy that the charge density in the case of the (OH···O) orientation is 0.025 a.u. This is significantly larger than the largest density in the (OH···Ar) orientation - which is 0.0074 a.u. However, for the OH···Ar orientation there are a larger number of smaller interactions between the hydroxyl hydrogen and the aromatic ring (Fig. 5). These numerous supplementary interactions may be one of the factors stabilizing the (OH···Ar) isomer.

3. Conclusion

Two new 1,3-thiazoles ***I*** and ***II*** were prepared via a

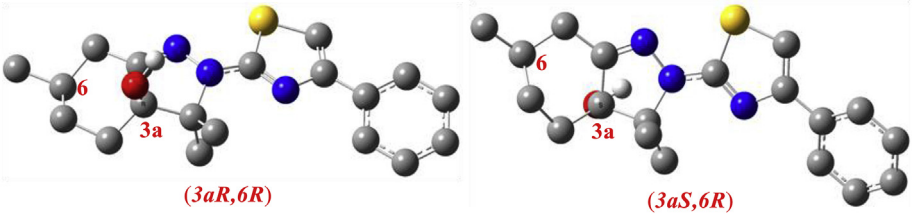

Fig. 3. Geometry optimized diastereomers of II.

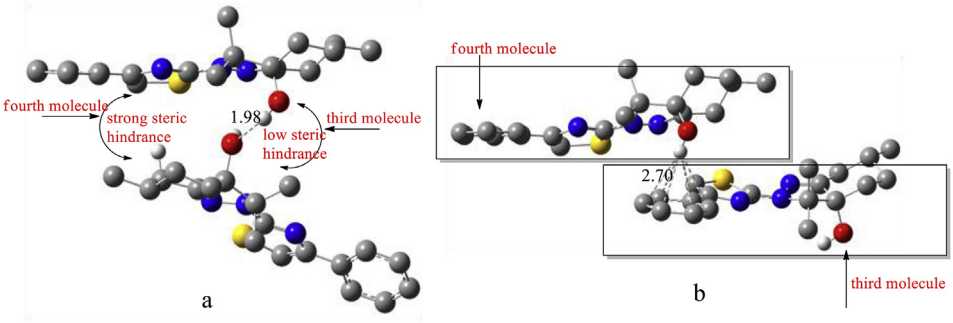

Fig. 4. The most stable dimers of (3aR,6R)-2-thiazolyl-indazole **II** optimized at the M052-X/6-31+G(d,p) level of theory. a: (OH···O) interaction, b: (OH···Ar) interaction.

Table 2
M052X/6-31+G(d,p) total (E, in a.u.), relative (ΔE, in kcal/mol) and binding (BE, in kcal/mol) energies of the two types of dimer of (*3aR,6R*)-2-Thiazolyl-Indazole ***II***.

Dimer	Gas phase			Ethanol		
	E[a]	ΔE[b]	BE	E[a]	ΔE[b]	BE
(OH···O)	−2750.193816	−0.68	−9.3	−2750.214244	−0.84	−7.0
(OH···Ar)	−2750.192738		−8.9	−2750.212907		−6.2

[a] Total energies are corrected by ZPE, which is scaled by the empirical factor of 0.961 and BSSE.
[b] ΔE = E((OH···O) - (OH···Ar)).

heterocyclization reaction of the corresponding monoterpenic thiosemicarbazones **2** and **3**, with phenacyl bromide **1**. Reaction with (R)-carvone thiosemicarbazone **2** yielded the expected 1,3-thiazole ***I***, while reaction with (R)-pulegone thiosemicarbazone **3**, yielded an unexpected indazolic thiazole ***II***. Both ***I*** and ***II*** were identified basing on their spectral data. An X-ray structural study was performed to elucidate the absolute configuration of ***II*** as (*3aR,6R*).

The crystallographic data suggested ready intermolecular interaction and polymerization between monomers of ***II***. To provide atomistic insight into this polymerization as well as understanding of the various structure features of the diastereomers of ***II***, we performed a computational quantum study of ***II*** and the dimer of ***II*** in the gas-phase and in solvent (ethanol). The computational results are in good agreement with the experimental observations. We see that the preferred diastereomer is (*3aR,6R*) and this isomer is favored by 4.5 kcal/mol. Two different types of hydrogen bonds can form between molecules of ***II*** via (OH···O) and (OH···Ar) interactions. The two modes of interaction are energetically similar with a small preference in favor of (OH···O). However, in the (OH···O) case, the polymerization of more than two molecules will produce unfavorable steric effects, unlike in the case of (OH···Ar), where the interaction is made in parallel planes and therefore has no steric hindrance. This may be the reason that the (OH···Ar) polymer is exclusively obtained experimentally.

4. Experimental section

All reagents and solvents were purchased from commercial sources (Aldrich, 112 Across) and used as received. Melting points (mp) were determined using a capillary apparatus and are uncorrected. Analytical thin-layer chromatography (TLC) was performed on plates percolated with E. Merck silica gel 60 F254 0.25 mm thick. ES-HRMS were obtained on a Q-TOF micromass spectrometer. NMR spectra were recorded on a Bruker AC 300 spectrometer at 300K. Samples were contained in 5 mm tubes and NMR spectra were measured at 300.13 MHz (^{1}H) and 75 MHz (^{13}C), with a concentration of 0.003 mol/L, in $CDCl_3$, in order to minimize the polymerization phenomenon. Chemical shifts (δ) are expressed in parts per million (ppm) with TMS as the internal standard. The general reproducibility of chemical shifts data was estimated to be better than ±0.01 ppm.

The monoterpenic thiosemicarbazones (**2** and **3**) were prepared by a condensation reaction of thiosemicarbazide respectively with naturally occurred (R)-carvone and (R)-pulegone according to the reported methods [29–33].

5. Computational details

All calculations were performed with the Gaussian 09 set of programs [34]. Geometry optimizations for all systems, both in gas phase and in ethanol as solvent, were performed using the M05-2X functional, which is known as a reliable DFT method that reproduces dispersion interactions well [35]. The basis set used was 6-31+G(d,p) [36]. In all cases, the analytical vibrational frequencies were computed to confirm that the optimized structures correspond to real minima on the potential energy surface. The corresponding zero point energy (ZPE) corrections were calculated for all optimized structures and scaled by the empirical factor 0.961 [23,37]

Calculations of nuclear shieldings were performed at the same level as the structural optimization, exploiting the gauge independent atomic orbital (GIAO) method [38,39]. Absolute isotropic magnetic shieldings were transformed into chemical shifts by reference to the shieldings of a standard compound (TMS) computed at the same level. To explore the influence of solvent on the structure and on chemical shifts we employed the PCM [40–43] model for ethanol as implemented in Gaussian 09. In this approach, the solute molecule is embedded in a cavity formed by the packet of spheres centred on solute atoms, the solvent is represented by an infinite dielectric medium characterized by the relative dielectric permittivity of the bulk, and the so called UAHF radii are used for building the effective cavity occupied by the solute in the solvent [44].

The interaction energies, in the case of dimers, have been corrected for basis set superposition errors (BSSE) by applying the counterpoise method of Boys and Bernardi [45]. The binding energies of the dimer, BE, were calculated as follows: $BE = E_D^{BSSE,ZPE} - 2(E_M^{ZPE})$, where $E_D^{BSSE,ZPE}$ is the total energy of the dimer corrected by BSSE and ZPE, and E_M^{ZPE} is the total energies of the isolated molecule corrected by the ZPE.

The charge distribution of the dimer in the case of (OH···O) and (OH···Ar) interactions, has been analyzed by means of the quantum theory of atoms in molecules (QTAIM) [46–48]. For each isomer we have constructed the molecular graph as the ensemble of bond critical points (BCPs) and bond paths. The electron density associated with a bonding critical point should be a good quantitative

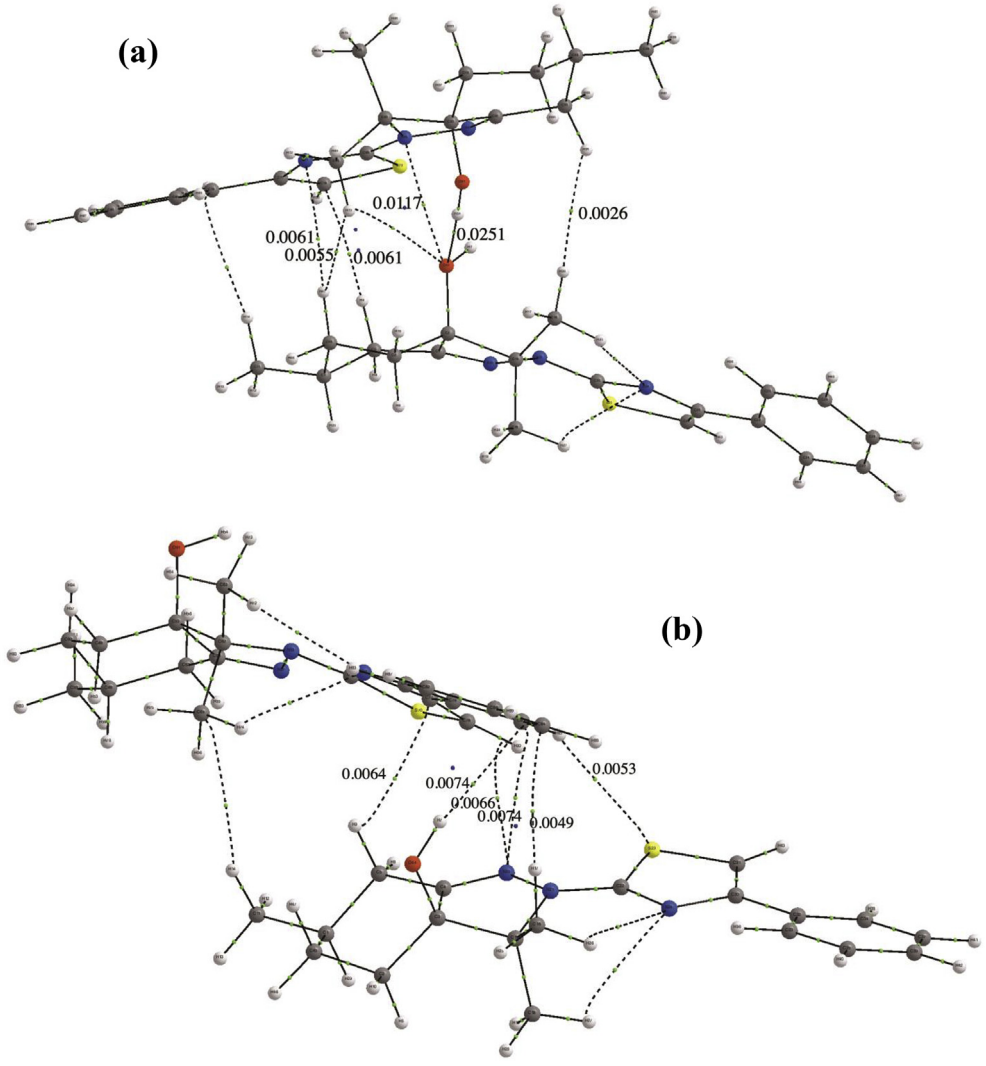

Fig. 5. Molecular graph for the interaction in the dimer (a): (OH···O) and (b): (OH···Ar). Green dots are bond critical points.

measurement of the strength of the linkage, but at the same time, the densities associated with the remainder of the system will provide useful information on the electron density redistribution upon interaction.

6. Synthesis

To a solution of thiosemicarbazones **2** or **3** (0.01 mol) and phenacyl bromide **1**(0.01 mol) in absolute ethanol (50 mL) was added (0.03 mol) of fused sodium acetate. The reaction mixture was heated under reflux for 1 h (The reaction progress was monitored by TLC). After evaporating the solvent, the residue was diluted with water (10 mL) and extracted with dichloromethane. The organic layer was separated, evaporated to dryness and then purified by silica gel column chromatography, using hexane/ethyl acetate as eluent, to obtain the corresponding 1,3-thiazoles in a pure quality.

6.1. (R)-2-(2-(5-isopropyl-2-methylcyclohex-2-enylidene) hydrazinyl)-4-phenylthiazole I

Yellow powder. Yield 98%, m.p. 242−243 °C (Ethanol).

FT-IR (KBr, νmax/cm^{-1}): 3416 (N-H); 3039 (Csp^2-H); 2929 (Csp^3-H); 1619(C═N); 1496 (N-H); 754 and 615 (MonosbstitutedAr); 887 (Csp^{2}H$_2$).

^{1}H-NMR (CDCl$_3$) δ ppm: 10.81 (brs,1H,NH); 7.70 (d (J = 7.55Hz), 2H, H-Ph), 7.26 (t (J = 7.55Hz), 2H, H-Ph); 7.21 (m, 1H, H-Ph); 6.71 (1H, s, H-thiazole); 5.92 (br s, 1H, H-C═C); 4.44 (s, 1H) and 4.60 (s, 1H) (H$_2$C═C); 2.08 (dd J = 16.09 and 2.48, 1H, one H of −CH$_2$-); 1.61−1.66 (m, 2H, -CH< and one H of −CH$_2$-); 2.04−2.09 (m, 2H, −CH$_2$-); 1.92 (s, 3H, CH$_3$); 1.55 (s, 3H, CH$_3$).

^{13}C-NMR (CDCl$_3$) δ ppm: 171.40 (-**C**═N); 151.26 (-**C**═N); 149.83 (N-**C** = thiazole); 147.27 (=**C**<); 131.58 (H**C** =); 134.97(=**C** < Ph); 132.53 (=**C**<); 128.52 (H**C**= Ph); 127.57 (H**C**= Ph); 126.06 (H**C**= Ph); 109.94 (H$_2$**C** =); 103.47 (H**C** = thiazole); 40.60 (-H**C**sp^3); 30.12(−CH$_2$-); 29.607 (−**C**H$_2$-); 20.42 (−**C**H$_3$); 17,71 (−**C**H$_3$).

HRMS (ES$^+$): m/z = 324.1530 [M+H]$^+$and calcd. mass 324.1534 [M+H]$^+$.

6.2. (3aR,6R)-3,3,6-trimethyl-2-(4-phenylthiazol-2-yl)-3,3a,4,5,6,7-hexahydro-2H-indazol-3a-olII

Green crystals. Yield 36%, m.p. 214−216 °C (Ethanol).

FT-IR (KBr, νmax/cm^{-1}): 3526 (OH); 3120 (Csp^2-H); 2970-2870 (Csp^3-H); 1537(C═N); 744 and 724 (Monosbstituted Ar); 776 (Csp^{2}H$_2$).

^{1}H NMR (CDCl$_3$) δ ppm: 7.87 (d J = 7.75Hz, 2H, H-Ph), 7.38

(t J = 7.75Hz, 2H, H-Ph); 7.27 (m, 1H, H-Ph); 6.85 (s, 1H, H-thiazole); 2.67 (1H, m, > CH-); 2.19 (dd J = 14.6 and 12.1Hz, 1H, one H of CH_2); 1.94 (s, 1H, OH exchangeable with D_2O); 1.88–1.56 (m, 5H, one H of CH_2- and $2CH_2$); 1.74 (s, 3H, CH_3); 1.36 (s, 3H, CH_3); 1.07 (d J = 6.05Hz, 3H, CH_3).

^{13}C-NMR ($CDCl_3$) δ ppm: 166.07 (-S-**C**=N- thiazole); 158.66 (-**C**=N-); 151.73 (N-**C** = thiazole); 135.26 (>**C**= Ph); 126,00 (=**C**H Ph); 127.61 (=**C**H Ph); 128.62(=**C**H Ph); 103.38 (=**C**H thiazole); 84.62 (>**C**-OH); 70.40 (>**C**<); 33.50 (>**C**H-); 33.18 (-$\mathbf{C}H_2$-); 31.06 (-$\mathbf{C}H_2$-); 29.56 (-$\mathbf{C}H_2$-); 22.16 (-$\mathbf{C}H_3$); 19.94 (-$\mathbf{C}H_3$); 19.20(-$\mathbf{C}H_3$).

HRMS (ES^+): m/z = 342.1635 $[M+H]^+$ and calculated mass 342.1640 [M+H]+.

Declaration of competing interest

The authors declare that they have no known competing financial interests or personal relationships that could have appeared to influence the work reported in this paper.

Acknowledgments

C.A.P. acknowledges support from the National Science Foundation (Grant CHE-1213271, CHE-18800014), the Donors of the American Chemical Society Petroleum Research Fund and the Floyd D. and Elisabeth S. Gottwald Endowment. The authors thank Professor A. Lamsabhi for AIM calculations.

Appendix A. Supplementary data

Supplementary data to this article can be found online at https://doi.org/10.1016/j.tet.2020.131830.

References

[1] A. Srinivas, Acta Chim. Slov. 63 (2016) 173–179.
[2] J. Quiroga, P. Hernández, B. Insuasty, R. Abonía, J. Cobo, A. Sánchez, M. Nogueras, J.N. Low, J. Chem. Soc. Perkin Trans. 1 (2002) 555–559.
[3] O. Uchikawa, K. Fukatsu, M. Suno, T. Aono, T. Doi, Chem. Pharmaceut. Bull. 44 (1996) 2070–2077.
[4] I. Akritopoulou-Zanze, B.D. Wakefield, A. Gasiecki, D. Kalvin, E.F. Johnson, P. Kovar, S.W. Djuric, Bioorg. Med. Chem. Lett 21 (2011) 1476–1479.
[5] M.G. Bursavich, D.P. Parker, J.A. Willardsen, Z.-H. Gao, T. Davis, K. Ostanin, R. Robinson, A. Peterson, D.M. Cimbora, J.-F. Zhu, B. Richards, Bioorg. Med. Chem. Lett 20 (2010) 1677–1679.
[6] M.V.N. de Souza, J. Sulfur Chem. 26 (2005) 429–449.
[7] M. Atobe, K. Naganuma, M. Kawanishi, A. Morimoto, K.-i. Kasahara, S. Ohashi, H. Suzuki, T. Hayashi, S. Miyoshi, Bioorg. Med. Chem. Lett 24 (2014) 1327–1333.
[8] P.L. Lobo, B. Poojary, M. Kumsi, V. Chandra, N.S. Kumari, K.R. Chandrashekar, Med. Chem. Res. 22 (2013) 1689–1699.
[9] B.N. Brousse, A.G. Moglioni, M.M. Alho, A. Alvarez-Larena, G.Y. Moltrasio, N.B. D'Accorso, Arkivoc 2002 (2002) 14–23.
[10] A. Feddouli, M.Y.A. Itto, M.A. Ali, A. Hasnaoui, A. Riahi, Synth. Commun. 36 (2006) 3617–3624.
[11] M.Y. Ait Itto, A. Feddouli, A. Boutalib, A. Riahi, J.-C. Daran, J. Sulfur Chem. 34 (2013) 250–258.
[12] A. Feddouli, M.Y.A. Itto, A. Hasnaoui, D. Villemin, P.-A. Jaffrès, J.S.-D.O. Santos, A. Riahi, F. Huet, J.-C. Daran, J. Heterocycl. Chem. 41 (2004) 731–735.
[13] A. N'Ait Ousidi, M.Y. Ait Itto, A. Auhmani, A. Riahi, A. Auhmani, J.-C. Daran, Acta Crystallogr. Sec. E Crystallogr. Commun. 73 (2017) 296–299.
[14] A.N. Ousidi, M.Y.A. Itto, A. Auhmani, Mustapha, Barakate, A. Riahi, H.B.E. Ayouchia, H. Anane, N.E. Aouad, M.A. Cruz, C. Díaz, IOSR J. Appl. Chem. 9 (2016) 52.
[15] L.R. Domingo, M. Ríos-Gutiérrez, P. Pérez, Org. Biomol. Chem. 18 (2020) 292–304.
[16] Bruker, APEX2, Bruker AXS Inc., Madison, Wisconsin USA, 2011.
[17] I.K. Boessenkool, J.C.A. Boeyens, J. Cryst. Mol. Struct. 10 (1980) 11–18.
[18] G.M. Sheldrick, Acta Crystallogr. Sec. C Struct. Chem. 71 (2015) 3–8.
[19] H.D. Flack, Acta Crystallogr. A Found. Crystallogr. 39 (1983) 876–881.
[20] M.N. Burnett, J.C.K. Ortepiii, Report ORNL-6895: USA, 1996.
[21] L.J. Farrugia, J. Appl. Crystallogr. 30 (1997), 565-565.
[22] A. Altomare, M.C. Burla, M. Camalli, G.L. Cascarano, C. Giacovazzo, A. Guagliardi, A.G.G. Moliterni, G. Polidori, R. Spagna, J. Appl. Crystallogr. 32 (1999) 115–119.
[23] A.P. Scott, L. Radom, J. Phys. Chem. 100 (1996) 16502–16513.
[24] M. Heger, J. Altnöder, A. Poblotzki, M.A. Suhm, Phys. Chem. Chem. Phys. 17 (2015) 13045–13052.
[25] G. Pietraperzia, M. Pasquini, F. Mazzoni, G. Piani, M. Becucci, M. Biczysko, D. Michalski, J. Bloino, V. Barone, J. Phys. Chem. 115 (2011) 9603–9611.
[26] J.T. Yi, J.W. Ribblett, D.W. Pratt, J. Phys. Chem. 109 (2005) 9456–9464.
[27] E. Calviño, M.C. Estañ, G.P. Simón, P. Sancho, M.d.C. Boyano-Adánez, E. de Blas, J. Bréard, P. Aller, Biochem. Pharmacol. 82 (2011) 1619–1629.
[28] I.H. Reece, R.L. Werner, Spectrochim. Acta Mol. Spectros 24 (1968) 1271–1282.
[29] Y. Sánchez, G.P. Simón, E. Calviño, E. de Blas, P. Aller, J. Pharmacol. Exp. Therapeut. 335 (2010) 114–123.
[30] P.J. Hesketh, D.R. Gandara, JNCI J. Natl. Canc. Inst. 83 (1991) 613–620.
[31] M. Aapro, Oncol. 9 (2004) 673–686.
[32] A.J. John, Heterocyclic Chemistry, fifth ed., 2010 fifth ed.
[33] G.N. Lipunova, E.V. Nosova, V.N. Charushin, O.N. Chupakhin, J. Fluor. Chem. 192 (2016) 1–21.
[34] R.A. Gaussian 09, M.J. Frisch, T. G W, H.B. Schlegel, G.E. Scuseria, M.A. Robb, J.R. C, G. Scalmani, V. Barone, B. Mennucci, G.A. Petersson, N. H, M. Caricato, X. Li, H.P. Hratchian, A.F. Izmaylov, B. J, G. Zheng, J.L. Sonnenberg, M. Hada, M. Ehara, T. K, R. Fukuda, J. Hasegawa, M. Ishida, T. Nakajima, Y. Honda, O. K, H. Nakai, T. Vreven, J.A. Montgomery Jr., J.E. Peralta, O. F, M. Bearpark, J.J. Heyd, E. Brothers, K.N. Kudin, V.N. S, R. Kobayashi, J. Normand, K. Raghavachari, A. R, J.C. Burant, S.S. Iyengar, J. Tomasi, M. Cossi, N. R, J.M. Millam, M. Klene, J.E. Knox, J.B. Cross, V. Bakken, C. A, J. Jaramillo, R. Gomperts, R.E. Stratmann, O. Yazyev, A.J. A, R. Cammi, C. Pomelli, J.W. Ochterski, R.L. Martin, M. K, V.G. Zakrzewski, G.A. Voth, P. Salvador, J.J. D, S. Dapprich, A.D. Daniels, O. Farkas, J.B. F, J.V. Ortiz, J. Cioslowski, D.J. Fox, G., Inc., Wallingford CT, 2009, p. 2009. Pittsburgh, PA.
[35] Y. Zhao, D.G. Truhlar, J. Phys. Chem. 110 (2006) 5121–5129.
[36] C. Lee, W. Yang, R.G. Parr, Phys. Rev. B 37 (1988) 785–789.
[37] I.M. Alecu, J. Zheng, Y. Zhao, D.G. Truhlar, J. Chem. Theor. Comput. 6 (2010) 2872–2887.
[38] R. Ditchfield, Mol. Phys. 27 (1974) 789–807.
[39] K. Wolinski, J.F. Hinton, P. Pulay, J. Am. Chem. Soc. 112 (1990) 8251–8260.
[40] R. Cammi, B. Mennucci, J. Tomasi, J. Phys. Chem. 103 (1999) 9100–9108.
[41] B. Mennucci, E. Cancès, J. Tomasi, J. Phys. Chem. B 101 (1997) 10506–10517.
[42] V. Barone, M. Cossi, J. Tomasi, J. Chem. Phys. 107 (1998) 3210.
[43] M. Cossi, G. Scalmani, N. Rega, V. Barone, J. Chem. Phys. 117 (2002) 43–54.
[44] H. Sasaki, S. Daicho, Y. Yamada, Y. Nibu, J. Phys. Chem. 117 (2013) 3183–3189.
[45] S.F. Boys, F. Bernardi, Mol. Phys. 19 (1970) 553–566.
[46] AIMAll, (Version 19.10.12), Todd A. Keith, TK Gristmill Software, Overland Park KS, USA, 2019 (aim.tkgristmill.com).
[47] C.F. Matta, R.J. Boyd, in: C.F. Matta, R.J. Boyd (Eds.), The Quantum Theory of Atoms in Molecules, Wiley-VCH Verlag GmbH & Co. KGaA, Weinheim, Germany, 2007, pp. 1–34.
[48] R.F.W. Bader, Atoms in Molecules: A Quantum Theory, Oxford University Press, Oxford, 1990.